Fluid Flow Around and Heat Transfer From an Infinite Circular Cylinder

W. A. Khan

J. R. Culham

M. M. Yovanovich

Microelectronics Heat Transfer Laboratory,
Department of Mechanical Engineering,
University of Waterloo,
Waterloo, Ontario, Canada N2L 3G1

In this study, an integral approach of the boundary layer analysis is employed to investigate fluid flow around and heat transfer from an infinite circular cylinder. The Von Karman–Pohlhausen method is used to solve momentum integral equation and the energy integral equation is solved for both isothermal and isoflux boundary conditions. A fourth-order velocity profile in the hydrodynamic boundary layer and a third-order temperature profile in the thermal boundary layer are used to solve both integral equations. Closed form expressions are obtained for the drag and the average heat transfer coefficients which can be used for a wide range of Reynolds and Prandtl numbers. The results for both drag and heat transfer coefficients are in good agreement with experimental/numerical data for a circular cylinder.
[DOI: 10.1115/1.1924629]

Introduction

The equations describing fluid flow and heat transfer in forced convection are complicated by being nonlinear. These nonlinearities arise from the inertial and convective terms in the momentum and energy equations, respectively. From a mathematical point of view, the presence of the pressure gradient term in the momentum equation for forced convection further complicates the problem. The energy equation depends on the velocity through the convective terms and, as a result, is coupled with the momentum equation.

Because of these mathematical difficulties, the theoretical investigations about fluid flow around and heat transfer from circular cylinders have mainly centered upon asymptotic solutions. These solutions are well documented in the open literature and are valid for very large ($>2\times10^5$) and small (<1) Reynolds numbers. However, no theoretical investigation could be found that can be used to determine drag coefficients and average heat transfer from cylinders for low to moderate Reynolds numbers ($1-2\times10^5$) as well as for large Prandtl numbers ($\geqslant 0.71$). For this range of Reynolds numbers and for selected fluids, there has been heavy reliance on both experiments and numerical methods. These approaches are not only expensive and time consuming but their results are applicable over a fixed range of conditions.

Unfortunately, many situations arise where solutions are required for low to moderate Reynolds numbers and for fluids having $\mathrm{Pr}>0.71$. Such solutions are of particular interest to thermal engineers involved with cylinders and fluids other than air or water. In this study a circular cylinder is considered in cross flow to investigate the fluid flow and heat transfer from a cylinder for a wide range of Reynolds and Prandtl numbers.

A review of existing literature reveals that most of the studies related to a single isolated cylinder are experimental or numerical. They are applicable over a fixed range of conditions. Furthermore, no analytical study gives a closed form solution for the fluid flow and heat transfer from a circular cylinder for a wide range of Reynolds and Prandtl numbers. At most, they provide a solution at the front stagnation point or a solution of boundary layer equations for very low Reynolds numbers. In this study, a closed form solution is obtained for the drag coefficients and Nusselt number, which can be used for a wide range of parameters. For this purpose, the Von Karman–Pohlhausen method is used, which was first introduced by Pohlhausen [1] at the suggestion of Von Karman [2] and then modified by Walz [3] and Holstein and Bohlen [4]. Schlichting [5] has explained and applied this method to the general problem of a two-dimensional boundary layer with pressure gradient. He obtained general solutions for the velocity profiles and the thermal boundary layers and compared them with the exact solution of a flat plate at zero incidence.

Analysis

Consider a uniform flow of a Newtonian fluid past a fixed circular cylinder of diameter D, with vanishing circulation around it, as shown in Fig. 1. The approaching velocity of the fluid is U_{app} and the ambient temperature is assumed to be T_a. The surface temperature of the wall is $T_w(>T_a)$ in the case of the isothermal cylinder and the heat flux is q for the isoflux boundary condition. The flow is assumed to be laminar, steady, and two-dimensional. The potential flow velocity just outside the boundary layer is denoted by $U(s)$. Using order-of-magnitude analysis, the reduced equations of continuity, momentum and energy in the curvilinear system of coordinates (Fig. 1) for an incompressible fluid can be written as:

Continuity:

$$\frac{\partial u}{\partial s}+\frac{\partial v}{\partial \eta}=0 \tag{1}$$

s-Momentum:

$$u\frac{\partial u}{\partial s}+v\frac{\partial u}{\partial \eta}=-\frac{1}{\rho}\frac{dP}{ds}+\nu\frac{\partial^2 u}{\partial \eta^2} \tag{2}$$

η-Momentum:

$$\frac{dP}{d\eta}=0 \tag{3}$$

Bernoulli equation:

$$-\frac{1}{\rho}\frac{dP}{ds}=U(s)\frac{dU(s)}{ds} \tag{4}$$

Energy:

$$u\frac{\partial T}{\partial s}+v\frac{\partial T}{\partial \eta}=\alpha\frac{\partial^2 T}{\partial \eta^2} \tag{5}$$

Hydrodynamic Boundary Conditions. At the cylinder surface, i.e., at $\eta=0$

$$u=0 \text{ and } \frac{\partial^2 u}{\partial \eta^2}=\frac{1}{\mu}\frac{\partial P}{\partial s} \tag{6}$$

At the edge of the boundary layer, i.e., at $\eta=\delta(s)$

$$u=U(s),\quad \frac{\partial u}{\partial \eta}=0 \text{ and } \frac{\partial^2 u}{\partial \eta^2}=0 \tag{7}$$

Contributed by the Heat Transfer Division for publication in the JOURNAL OF HEAT TRANSFER. Manuscript received May 25, 2004. Final manuscript received October 25, 2004. Review conducted by: N. K. Anand.

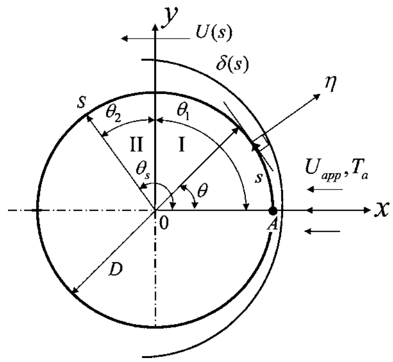

Fig. 1 Flow over a circular cylinder

Thermal Boundary Conditions. The boundary conditions for the uniform wall temperature (UWT) and uniform wall flux (UWF) are:

$$\eta=0,\quad \begin{cases} T=T_w & \text{for UWT} \\ \dfrac{\partial T}{\partial \eta}=-\dfrac{q}{k_f} & \text{for UWF} \end{cases} \tag{8}$$

$$\eta=\delta_T,\quad T=T_a \text{ and } \frac{\partial T}{\partial \eta}=0 \tag{9}$$

Velocity Distribution. Assuming a thin boundary layer around the cylinder, the velocity distribution in the boundary layer can be approximated by a fourth order polynomial as suggested by Pohlhausen [1]:

$$\frac{u}{U(s)}=(2\eta_H-2\eta_H^3+\eta_H^4)+\frac{\lambda}{6}(\eta_H-3\eta_H^2+3\eta_H^3-\eta_H^4) \tag{10}$$

where $0 \leqslant \eta_H=\eta/\delta(s) \leqslant 1$ and λ is the pressure gradient parameter, given by

$$\lambda=\frac{\delta^2}{\nu}\frac{dU(s)}{ds} \tag{11}$$

With the help of velocity profiles, Schlichting [5] showed that the parameter λ is restricted to the range $-12 \leqslant \lambda \leqslant 12$.

Temperature Distribution. Assuming a thin thermal boundary layer around the cylinder, the temperature distribution in the thermal boundary layer can be approximated by a third order polynomial

$$\frac{T-T_a}{T_w-T_a}=1-\frac{3}{2}\eta_T+\frac{1}{2}\eta_T^3 \tag{12}$$

for the isothermal boundary condition and

$$T-T_a=\frac{2q\delta_T}{3k_f}\left(1-\frac{3}{2}\eta_T+\frac{1}{2}\eta_T^3\right) \tag{13}$$

for the isoflux boundary condition.

Boundary Layer Parameters. In dimensionless form, the momentum integral equation can be written as

$$\frac{U\delta_2}{\nu}\frac{d\delta_2}{ds}+\left(2+\frac{\delta_1}{\delta_2}\right)\frac{\delta_2^2}{\nu}\frac{dU}{ds}=\frac{\delta_2}{U}\left.\frac{\partial u}{\partial \eta}\right|_{\eta=0} \tag{14}$$

where δ_1 and δ_2 are the displacement and momentum boundary layer thicknesses.

By solving the momentum integral equation, Khan [6] obtained the local dimensionless boundary layer and momentum thicknesses:

$$\frac{\delta}{D}=\frac{0.5}{\sqrt{\mathrm{Re}_D}}\sqrt{\frac{\lambda}{\cos\theta}} \tag{15}$$

$$\frac{\delta_2}{D}=\frac{0.3428}{\sqrt{\mathrm{Re}_D}}\sqrt{\frac{1}{\sin^6\theta}\int_0^\theta \sin^5\zeta d\zeta} \tag{16}$$

where Re_D is the Reynolds number, defined as

$$\mathrm{Re}_D=\frac{U_{\mathrm{app}}D}{\nu} \tag{17}$$

and λ is the pressure gradient parameter, whose values are obtained corresponding to each position along the cylinder surface. These values were fitted by the least squares method and given by Khan [6]. Using analytical definition of the point of separation, Khan [6] obtained the angle of separation as $\theta_s=107.71$ deg, that depends on the velocity distribution inside the boundary layer. This angle of separation is in close agreement with Schöenauer [7] (=104.5 deg), Schlichting [5] (109.5 deg), Žukauskas and Žiugžda [8] (105 deg) and Churchill [9] (108.8 deg).

Fluid Flow. The first parameter of interest is fluid friction which manifests itself in the form of the drag force F_D, where F_D is the sum of the skin friction drag D_f and pressure drag D_p. Skin friction drag is due to viscous shear forces produced at the cylinder surface, predominantly in those regions where the boundary layer is attached. In dimensionless form, it can be written as

$$C_f=\frac{\tau_w}{\frac{1}{2}\rho U_{\mathrm{app}}^2}=\frac{4}{3}\frac{\lambda+12}{\sqrt{\mathrm{Re}_D}}\sin\theta\sqrt{\frac{\cos\theta}{\lambda}} \tag{18}$$

The friction drag coefficient can be defined as

$$C_{Df}=\int_0^\pi C_f\sin\theta d\theta=\int_0^{\theta_s} C_f\sin\theta d\theta+\int_{\theta_s}^\pi C_f\sin\theta d\theta \tag{19}$$

Since the shear stress on the cylinder surface after boundary layer separation is negligible, the second integral will be zero and the friction drag coefficient can be written as

$$C_{Df}=\int_0^{\theta_s} C_f\sin\theta d\theta=\frac{5.786}{\sqrt{\mathrm{Re}_D}} \tag{20}$$

Pressure drag is due to the unbalanced pressures which exist between the relatively high pressures on the upstream surfaces and the lower pressures on the downstream surfaces. In dimensionless form, it can be written as

$$C_{Dp}=\int_0^\pi C_p\cos\theta d\theta \tag{21}$$

where C_p is the pressure coefficient and can be defined as

$$C_p=\frac{\Delta P}{\frac{1}{2}\rho U_{\mathrm{app}}^2} \tag{22}$$

The pressure difference ΔP can be obtained by integrating θ-momentum equation with respect to θ. In dimensionless form, it can be written as

$$\frac{\Delta P}{\frac{1}{2}\rho U_{\mathrm{app}}^2}=2(1-\cos\theta)+\frac{8}{\mathrm{Re}_D}(1-\cos\theta) \tag{23}$$

So, the pressure drag coefficient for the cylinder up to the separation point will be

$$C_{Dp}=\int_0^{\theta_s} C_p\cos\theta d\theta=1.152+\frac{1.26}{\mathrm{Re}_D} \tag{24}$$

The total drag coefficient C_D can be written as the sum of both drag coefficients

$$C_D = \frac{5.786}{\sqrt{\mathrm{Re}_D}} + 1.152 + \frac{1.26}{\mathrm{Re}_D} \tag{25}$$

which was also obtained by Khan et al. [10] as a limiting case of an elliptical cylinder.

Heat Transfer. The second parameter of interest in this study is the dimensionless average heat transfer coefficient, Nu_D for large Prandtl numbers ($\geqslant 0.71$). This parameter is determined by integrating Eq. (5) from the cylinder surface to the thermal boundary layer edge. Assuming the presence of a thin thermal boundary layer δ_T along the cylinder surface, the energy integral equation for the isothermal boundary condition can be written as

$$\frac{d}{ds}\int_0^{\delta_T} (T - T_a) u \, d\eta = -\alpha \left. \frac{\partial T}{\partial \eta} \right|_{\eta=0} \tag{26}$$

Using velocity and temperature profiles Eqs. (10) and (12), and assuming $\zeta = \delta_T/\delta < 1$, Eq. (26) can be simplified to

$$\delta_T \frac{d}{ds}[U(s)\delta_T \zeta(\lambda + 12)] = 90\alpha \tag{27}$$

This equation can be rewritten separately for the two regions (Fig. 1), i.e.

$$\delta_T \frac{d}{ds}[U(s)\delta_T \zeta(\lambda_1 + 12)] = 90\alpha \tag{28}$$

for region I, and

$$\delta_T \frac{d}{ds}[U(s)\delta_T \zeta(\lambda_2 + 12)] = 90\alpha \tag{29}$$

for region II. Integrating Eqs. (28) and (29), in the respective regions, with respect to s, one can obtain local thermal boundary layer thicknesses

$$\left(\frac{\delta_T(\theta)}{D}\right) \cdot \mathrm{Re}_D^{1/2}\,\mathrm{Pr}^{1/3} = \begin{cases} \sqrt[3]{\dfrac{45 f_1(\theta)}{2(\lambda_1 + 12)^2 \sin^2\theta}\sqrt{\dfrac{\lambda_1}{\cos\theta}}} & \text{for region I} \\ \sqrt[3]{\dfrac{45 f_3(\theta)}{2\sin^2\theta}\sqrt{\dfrac{\lambda_2}{\cos\theta}}} & \text{for region II} \end{cases} \tag{30}$$

where the functions $f_1(\theta)$ and $f_3(\theta)$ are given by

$$f_1(\theta) = \int_0^{\theta} \sin\theta(\lambda_1 + 12)\, d\theta \tag{31}$$

and

$$f_3(\theta) = \frac{f_1(\theta)}{\lambda_1 + 12} + \frac{f_2(\theta)}{\lambda_2 + 12} \tag{32}$$

with

$$f_2(\theta) = \int_{\theta_1}^{\theta_s} \sin\theta(\lambda_2 + 12)\, d\theta \tag{33}$$

The local heat transfer coefficients, for the isothermal boundary condition, in both the regions can be written as

$$h_1(\theta) = \frac{3k_f}{2\delta_{T_1}} \text{ and } h_2(\theta) = \frac{3k_f}{2\delta_{T_2}} \tag{34}$$

Thus the dimensionless local heat transfer coefficients, for both the regions, can be written as

$$\frac{\mathrm{Nu}_D(\theta)|_{\mathrm{isothermal}}}{\mathrm{Re}_D^{1/2}\,\mathrm{Pr}^{1/3}} = \begin{cases} \dfrac{3}{2}\sqrt[3]{\dfrac{2(\lambda_1 + 12)^2 \sin^2\theta}{45 f_1(\theta)}\sqrt{\dfrac{\cos\theta}{\lambda_1}}} & \text{for region I} \\ \dfrac{3}{2}\sqrt[3]{\dfrac{2\sin^2\theta}{45 f_3(\theta)}\sqrt{\dfrac{\cos\theta}{\lambda_2}}} & \text{for region II} \end{cases} \tag{35}$$

The average heat transfer coefficient is defined as

$$h = \frac{1}{\pi}\int_0^{\pi} h(\theta)\, d\theta = \frac{1}{\pi}\left\{\int_0^{\theta_s} h(\theta)\, d\theta + \int_{\theta_s}^{\pi} h(\theta)\, d\theta\right\} \tag{36}$$

The integral analysis is unable to predict heat transfer values from separation point to the rear stagnation point. However, experiments (Žukauskas and Žiugžda [8], Fand and Keswani [11], and Nakamura and Igarashi [12] among others) show that, the heat transfer from the rear portion of the cylinder increases with Reynolds numbers. From a collection of all known data, Van der Hegge Zijnen [13] demonstrated that the heat transferred from the rear portion of the cylinder can be determined from $\mathrm{Nu}_D = 0.001\,\mathrm{Re}_D$ that shows the weak dependence of average heat transfer from the rear portion of the cylinder on Reynolds numbers. In order to include the share of heat transfer from the rear portion of the cylinder, the local heat transfer coefficients are integrated upto the separation point and averaged over the whole surface, that is

$$h = \frac{1}{\pi}\int_0^{\theta_s} h(\theta)\, d\theta = \frac{1}{\pi}\left\{\int_0^{\theta_1} h_1(\theta)\, d\theta + \int_{\theta_1}^{\theta_s} h_2(\theta)\, d\theta\right\} \tag{37}$$

Using Eqs. (30)–(34), Eq. (37) can be solved for the average heat transfer coefficient which gives the average Nusselt number for an isothermal cylinder as

$$\mathrm{Nu}_D|_{\mathrm{isothermal}} = 0.593\,\mathrm{Re}_D^{1/2}\,\mathrm{Pr}^{1/3} \tag{38}$$

For the isoflux boundary condition, the energy integral equation can be written as

$$\frac{d}{ds}\int_0^{\delta_T} (T - T_a) u \, d\eta = \frac{q}{\rho c_p} \tag{39}$$

Assuming constant heat flux and thermophysical properties, Eq. (39) can be simplified to

$$\frac{d}{ds}[U(s)\delta_T^2 \zeta(\lambda + 12)] = 90\frac{\nu}{\mathrm{Pr}} \tag{40}$$

Rewriting Eq. (40) for the two regions in the same way as Eq. (27), one can obtain local thermal boundary layer thicknesses δ_{T_1} and δ_{T_2} under isoflux boundary condition. The local surface temperatures for the two regions can then be obtained from temperature distribution

$$\Delta T_1(\theta) = \frac{2q\delta_{T_1}}{3k_f} \tag{41}$$

and

$$\Delta T_2(\theta) = \frac{2q\delta_{T_2}}{3k_f} \tag{42}$$

The local heat transfer coefficient can now be obtained from its definition as

$$h_1(\theta) = \frac{q}{\Delta T_1(\theta)} \quad \text{and} \quad h_2(\theta) = \frac{q}{\Delta T_2(\theta)} \tag{43}$$

which give the local Nusselt numbers for the cross flow over a cylinder with constant flux

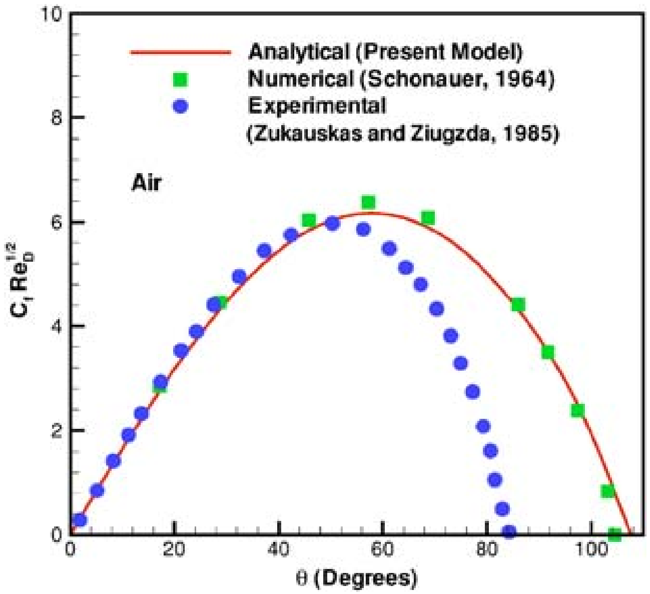

Fig. 2 Distribution of shear stress on a circular cylinder in air

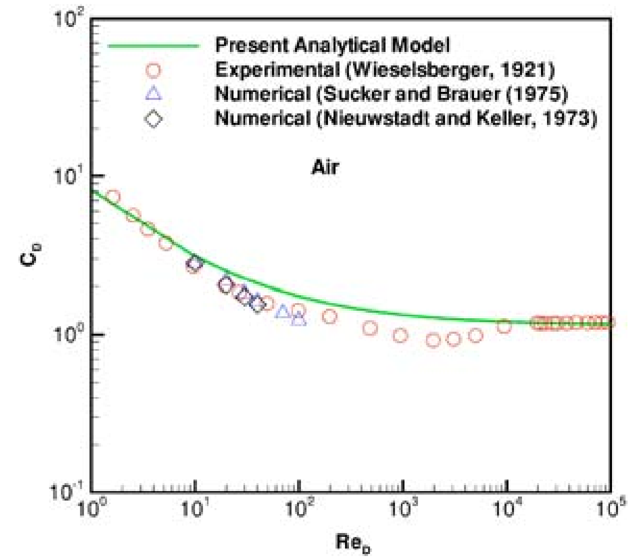

Fig. 3 Drag coefficient as a function of Re_D for a circular cylinder

$$\frac{Nu_D(\theta)|_{\mathrm{isoflux}}}{Re_D^{1/2}\,Pr^{1/3}}=\begin{cases}\dfrac{3}{2}\sqrt[3]{\dfrac{4(\lambda_1+12)\sin\theta}{45f_4(\theta)}}\sqrt{\dfrac{\cos\theta}{\lambda_1}} & \text{for region I}\\[2ex] \dfrac{3}{2}\sqrt[3]{\dfrac{4\sin\theta}{45f_6(\theta)}}\sqrt{\dfrac{\cos\theta}{\lambda_2}} & \text{for region II}\end{cases} \tag{44}$$

Following the same procedure for the average heat transfer coefficient as mentioned above, one can obtain the average Nusselt number for an isoflux cylinder as

$$Nu_D|_{\mathrm{isoflux}}=0.632\,Re_D^{1/2}\,Pr^{1/3} \tag{45}$$

This Nusselt number is 6% greater than the average Nusselt number for an isothermal cylinder. Combining the results for both thermal boundary conditions, we have

$$\frac{Nu_D}{Re_D^{1/2}\,Pr^{1/3}}=\begin{cases}0.593 & \text{for UWT}\\ 0.632 & \text{for UWF}\end{cases} \tag{46}$$

The same values were obtained by Khan [10] as a limiting case of an elliptical cylinder.

Results and Discussion

Flow Characteristics. The dimensionless local shear stress, $C_f\sqrt{Re_D}$, is plotted in Fig. 2. It can be seen that C_f is zero at the stagnation point and reaches a maximum at $\theta \approx 58$ deg. The increase in shear stress is caused by the deformation of the velocity profiles in the boundary layer, a higher velocity gradient at the wall and a thicker boundary layer. In the region of decreasing C_f preceeding the separation point, the pressure gradient decreases further and finally C_f falls to zero at $\theta = 107.7°$, where boundary-layer separation occurs. Beyond this point, C_f remains close to zero up to the rear stagnation point. These results are compared with the experimental results of Žukauskas and Žiugžda [8] and the numerical data of Schönauer [7]. Schönauer [7] data is in good agreement for the entire range, whereas, Žukauskas and Žiugžda [8] results are in good agreement for the front part of the cylinder only. This is probably due to high Reynolds numbers used in experiments.

The variation of the total drag coefficient C_D with Re_D is illustrated in Fig. 3 for an infinite cylinder in air. The present results are compared with the experimental results of Wieselsberger [14] as well as numerical data of Sucker and Brauer [15] and Niuwstadt and Keller [16]. The present results are in good agreement except at $Re_D = 2\times 10^3$, where a downward deviation (23.75%) in the experimental results was noticed. No physical explanation could be found in the literature for this deviation.

Heat Transfer Characteristics. The comparison of local Nusselt numbers for the isothermal and isoflux boundary conditions is presented in Fig. 4. The isoflux boundary condition gives a higher heat transfer coefficient over the larger part of the circumference. On the front part of the cylinder (up to $\theta \approx 30$ deg), there is no appreciable effect of boundary condition. Empirical correlation of Kreith [17] as well as experimental data of Nakamura and Igarashi [12], van Meel [18] and Giedt [19] are also plotted to compare the analytical distribution of local heat transfer coefficients for isothermal boundary condition. The integral analysis of the boundary layer gives higher local heat transfer coefficients (around 15%)

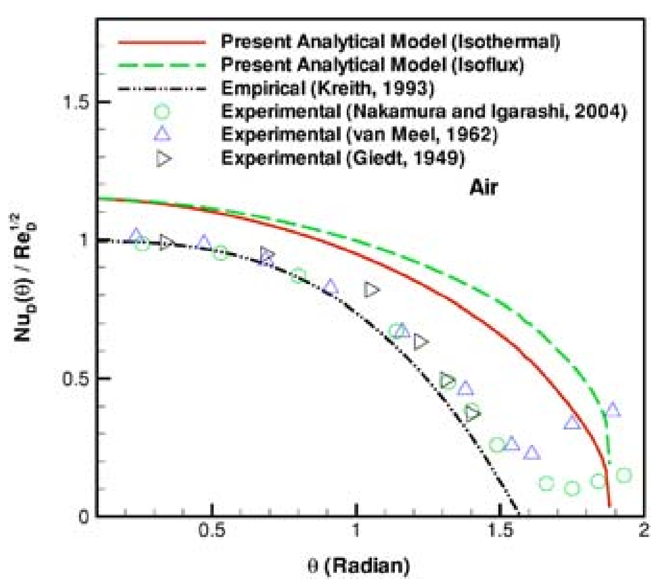

Fig. 4 Local Nusselt numbers for different boundary conditions

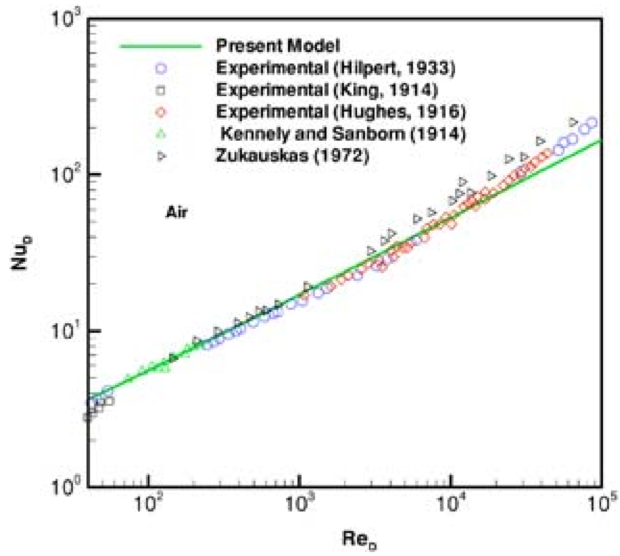

Fig. 5 Variation of average Nusselt number with Reynolds number for isothermal boundary condition

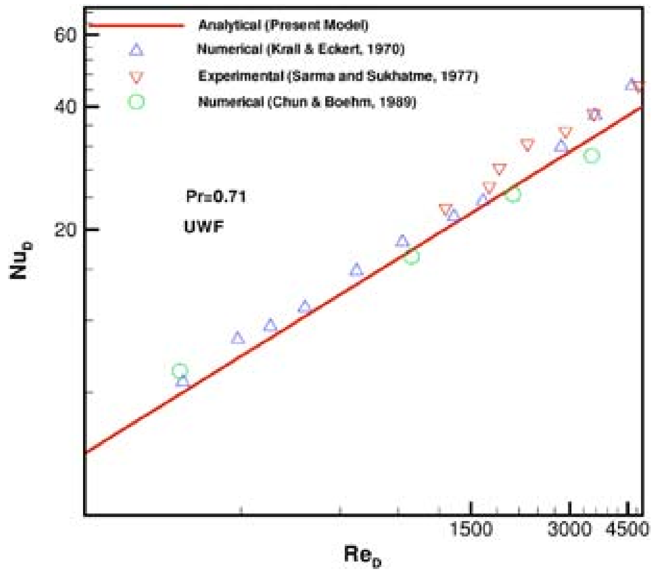

Fig. 6 Variation of average Nusselt number with Reynolds number for isoflux boundary condition

over the entire circumference of the cylinder. This discrepancy is probably due to the assumed velocity and temperature profiles in the boundary layer.

The results of heat transfer from a single isothermal cylinder are shown in Fig. 5, where they are compared with the experimental data of Hilpert [20], King [21], Hughes [22], Kennely and Sanborn [23], and Žukauskas [24]. Good agreement is observed in the entire laminar flow range except in the subcritical range. The discrepancy increases as the Reynolds number increases. This discrepancy is probably due to the effect of free-stream turbulence or vortex shedding in actual experiments. It was demonstrated by Kestin [25], Smith and Kuethe [26], Dyban and Epick [27], and Kestin and Wood [28] that the heat transfer coefficient increases with turbulence intensity and that this effect is more intense when the Reynolds number is higher. In the present analysis these effects are not included, so the discrepancy can be observed clearly in Fig. 5 for higher Reynolds numbers. Average Nusselt numbers for the isoflux boundary condition are compared in Fig. 6 with the experimental/numerical results. The average Nu_D values are found to be in a good agreement with both numerical results of Krall and Eckert [29] and Chun and Boehm [30]. However, the experimental results of Sarma and Sukhatme [31] are found to be higher ($\approx 8\%$).

Summary

An integral approach is employed to investigate the fluid flow and heat transfer from an isolated circular cylinder. Closed form solutions are developed for both the drag and heat transfer coefficients in terms of Reynolds and Prandtl numbers. The correlations of heat transfer are developed for both isothermal and isoflux boundary conditions. It is shown that the present results are in good agreement with the experimental results for the full laminar range of Reynolds numbers in the absence of free stream turbulence and blockage effects.

Acknowledgments

The authors gratefully acknowledge the financial support of Natural Sciences and Engineering Research Council of Canada and the Center for Microelectronics Assembly and Packaging.

Nomenclature

C_D = total drag coefficient
C_{Df} = friction drag coefficient
C_{Dp} = pressure drag coefficient
C_f = skin friction coefficient $\equiv 2\tau_w/\rho U_{\mathrm{app}}^2$
C_p = pressure coefficient $\equiv 2\Delta P/\rho U_{\mathrm{app}}^2$
c_p = specific heat of the fluid (J/kg K)
D = cylinder diameter (m)
k = thermal conductivity (W/m K)
h = average heat transfer coefficient (W/m^2 K)
Nu_D = average Nusselt number based on the diameter of the cylinder $\equiv hD/k_f$
Pr = Prandtl number $\equiv \nu/\alpha$
P = pressure (N/m^2)
q = heat flux (W/m^2)
Re_D = Reynolds number based on the diameter of the cylinder $\equiv DU_{\mathrm{app}}/\nu$
s = distance along the curved surface of the circular cylinder measured from the forward stagnation point (m)
T = temperature (C)
U_{app} = approach velocity (m/s)
$U(s)$ = potential flow velocity just outside the boundary layer $\equiv 2U_{\mathrm{app}} \sin\theta$ (m/s)
u = s-component of velocity in the boundary layer (m/s)
v = η-component of velocity in the boundary layer (m/s)

Greek Symbols

α = thermal diffusivity (m^2/s)
δ = hydrodynamic boundary-layer thickness (m)
δ_1 = displacement thickness (m)
δ_2 = momentum thickness (m)
δ_T = thermal boundary layer thickness (m)
η = distance normal to and measured from the surface of the circular cylinder (m)
λ = pressure gradient parameter
μ = absolute viscosity of the fluid (N s/m^2)
ν = kinematic viscosity of the fluid (m^2/s)
ρ = density of the fluid (kg/m^3)
τ = shear stress (N/m^2)
θ = angle measured from front stagnation point (rad)

ζ = ratio of thermal and hydrodynamic boundary layers $\equiv \delta_T/\delta$

Subscripts

a = ambient
f = fluid or friction
H = hydrodynamic
p = pressure
s = separation
T = thermal or temperature
w = wall

References

[1] Pohlhausen, K., 1921, "Zur Näherungsweise Integration der Differential Gleichung der Laminaren Reibungschicht," Z. Angew. Math. Mech., **1**, pp. 252–268.

[2] Von Karman, T., 1921, "Über Laminar Und Turbulente Reibung," Z. Angew. Math. Mech., **1**, pp. 233–252.

[3] Walz, A., 1941, "Ein neuer Ansatz für das Greschwindligkeitsprofil der laminaren Reibungsschicht," Lilienthal-Bericht, **141**, p. 8.

[4] Holstein, H., and Bohlen, T., 1950, "Ein einfaches Verfahren zur Berechnung Laminaren Reibungsschichten," die dem Nahenungsansatz von K. Pohlhausen genugen, Lilenthal Bericht, **510**, p. 5.

[5] Schlichting, H., 1979, *Boundary Layer Theory*, 7th ed., McGraw–Hill, New York.

[6] Khan, W. A., 2004, "Modeling of Fluid Flow and Heat Transfer for Optimization of Pin-Fin Heat Sinks," Ph.D. thesis, Department of Mechanical Engineering, University of Waterloo, Canada.

[7] Schönauer, W., 1964, "Ein Differenzenverfahren zur Lösung der Grenzschichtgleichung für stationäre, laminare, inkompressible Strömung," Ing.-Arch., **33**, p. 173.

[8] Žukauskas, A., and Žiugžda, J., 1985, *Heat Transfer of a Cylinder in Crossflow*, Hemisphere, New York.

[9] Churchill, S. W., 1988, *Viscous Flows: The Practical Use of Theory*, Butterworths Series in Chemical Engineering, USA, pp. 317–358.

[10] Khan, W. A., Culham, J. R., and Yovanovich, M. M., 2005, "Fluid Flow and Heat Transfer from Elliptical Cylinders," J. Thermophys. Heat Transfer, **19**(2), pp. 178-185; also presented at AIAA 37th Thermophysics Conference, Portland, OR, June 29–July 1, 2004.

[11] Fand, R. M., and Keswani, K. K., 1972, "A Continuous Correlation Equation for Heat Transfer From Cylinders to Air in Crossflow for Reynolds Numbers From 10^{-2} to 2×10^5," Int. J. Heat Mass Transfer, **15**, pp. 559–562.

[12] Nakamura, H., and Igarashi, T., 2004, "Variation of Nusselt Number with Flow Regimes Behind a Circular Cylinder for Reynolds Numbers from 70 30000," Int. J. Heat Mass Transfer, **47**, pp. 5169–5173.

[13] Van der Hegge Zijnen, B. G., 1956, "Modified Correlation Formulae for Heat Transfer by Natural and Forced Convection from Horizontal Cylinders," Appl. Sci. Res., Sect. A, **6**, No. 2–3, pp. 129–140.

[14] Wieselsberger, C., 1921, "New Data on The Laws of Fluid Resistance," NACA TN No. 84.

[15] Sucker, D., and Brauer, H., 1995, "Investigation of the Flow Around Transverse Cylinders," Thermo and Fluid Dynamics, **8**, pp. 149–158.

[16] Nieuwstadt, F., and Keller, H. B., 1973, "Viscous Flow Past Circular Cylinders," Comput. Fluids, **1**, pp. 59.

[17] Kreith, F., and Bohn, M. S., 1993, *Principles of Heat Transfer*, 5th ed., West Publishing Company, New York, pp. 469–485.

[18] van Meel, D. A., 1962, "A Method for the Determination of Local Convective Heat Transfer from a Cylinder Placed Normal to an Air Stream," Int. J. Heat Mass Transfer, **5**, pp. 715–722.

[19] Giedt, W. H., 1949, "Investigation of Variation of Point Unit Heat-Transfer Coefficient Around a Cylinder Normal to an Air Stream," Trans. ASME, **71**, pp. 375–381.

[20] Hilpert, R., 1933, "Experimental Study of Heat Dissipation of Heated Wire and Pipe in Air Current," Forschungsarbeiten auf dem Gebiete des Ingenieurwesens - Ausgabe A, **4**(5), pp. 215–224.

[21] King, L. V., 1914, "The Convection of Heat from Small Cylinders in a Stream of Fluid: Determination of the Convection Constants of Small Platinum Wires with Applications to Hot-Wire Anemometry," Philos. Trans. R. Soc. London, Ser. A, **214**, pp. 373–433.

[22] Hughes, J. A., 1916, "The Cooling of Cylinders in a Stream of Air," Philos. Mag., **31**, pp. 118–130.

[23] Kennely, A. E., and Sanborn, H. S., 1914, "The Influence of Atmospheric Pressure Upon the Forced Thermal Convection from Small Electrically Heated Platinum Wires," Proceedings of the American Philosophical Society, Vol. 53, pp. 55–77.

[24] Žukauskas, A., 1972, *Advances in Heat Transfer*, Academic Press, New York, pp. 93–160.

[25] Kestin, J., 1966, "The Effect of Free Stream Turbulence on Heat Transfer Rates," *Advances in Heat Transfer*, Academic Press, New York, Vol. 3, pp. 1–32.

[26] Smith, M. C., and Kuethe, A. M., 1966, "Effects of Turbulence on Laminar Skin Friction and Heat Transfer," Phys. Fluids, **9**, pp. 2337–2344. *Advances in Heat Transfer*, Academic Press, New York, Vol. 3, pp. 1–32.

[27] Dyban, E. P., and Epick, E. Ya., 1970, "Some Heat Transfer Features in the Air Flows of Intensified Turbulence," in Proceedings of 4th Heat Transfer Conference, F. C. 5.7, Part 2, Paris-Versailles.

[28] Kestin, J., and Wood, R. T., 1971, "The Influence of Turbulence on Mass Transfer from Cylinders," *Advances in Heat Transfer*, Academic Press, New York, Vol. 3, pp. 1–32.

[29] Krall, K. M., and Eckert, E. R. G., 1970, "Heat Transfer to a Transverse Circular Cylinder at Low Reynolds Number Including Refraction Effects," Heat Transfer-Sov. Res., **3**, pp. 225–232.

[30] Chun, W., and Boehm, R. F., 1989, "Calculation of Forced Flow and Heat Transfer Around a Cylinder in Cross Flow," Numer. Heat Transfer, Part A, **15**(1), pp. 101–122.

[31] Sarma, T. S., and Sukhatme, S. P., 1977, "Local Heat Transfer from a Horizontal Cylinder to Air in Cross Flow: Influence of Free Convection and Free Stream Turbulence," Int. J. Heat Mass Transfer, **20**, pp. 51–56.